Hindawi
Complexity
Volume 2020, Article ID 2941809, 14 pages
https://doi.org/10.1155/2020/2941809

Research Article

Load Estimation of Complex Power Networks from Transformer Measurements and Forecasted Loads

Haina Rong[1] **and Francisco de León**[2]

[1]*School of Electrical Engineering, Southwest Jiaotong University, Chengdu 610031, China*
[2]*Department of Electrical and Computer Engineering, New York University, Five Metrotech Center, Brooklyn, NY 11201, USA*

Correspondence should be addressed to Haina Rong; ronghaina@126.com

Received 24 August 2019; Revised 17 December 2019; Accepted 2 January 2020; Published 22 January 2020

Academic Editor: Zhile Yang

This paper presents a load estimation method applicable to complex power networks (namely, heavily meshed secondary networks) based on available network transformer measurements. The method consists of three steps: network reduction, load forecasting, and state estimation. The network is first mathematically reduced to the terminals of loads and measurement points. A load forecasting approach based on temperature is proposed to solve the network unobservability. The relationship between outdoor temperature and power consumption is studied. A power-temperature curve, a nonlinear function, is obtained to forecast loads as the temperature varies. An "effective temperature" reflecting complex weather conditions (sun irradiation, humidity, rain, etc.) is introduced to properly consider the effect on the power consumption of cooling and heating devices. State estimation is adopted to compute loads using network transformer measurements and forecasted loads. Experiments conducted on a real secondary network in New York City with 1040 buses verify the effectiveness of the proposed method.

1. Introduction

Power networks are one kind of the most complex artificial network in the world. Load estimation has long been an important issue in electrical power systems for energy management and operation. Differing from load forecasting aiming for offline studies with mainly historical data, load estimation usually aims to obtain real-time load data by using two kinds of measurements: real-time measurements and load pseudomeasurements resulting from monthly billing data, monthly peak load readings, transformers peak load analysis, and existing diversified load curves [1, 2]. In power systems, loads of an observable network can be estimated using state estimation (SE) methods, which are widely utilized since their introduction to transmission systems in 1968 [3–8]. The basic idea of SE is to compute the unknowns through available redundant measurements [9, 10]. These measurements could be voltage, phase, power injection, power flow, or current from substations, generators, or transformers [11, 12]. However, the required measurements are not usually enough to satisfy the network observability.

Network unobservability can be solved by adding more measurements or pseudomeasurements. Extra measurements can be obtained by installing more monitors (or meters) in an electrical network. The more devices are installed, the better accuracy of the estimated values would be obtained. Supervisory control and data acquisition (SCADA) systems [9–15] or phasor measurement units (PMUs) [14–18] are often installed to provide enough measurements. However, device installation is not always possible due to various reasons, in particular high cost. Under this condition, pseudomeasurements, which could be a forecasted value derived from historical data or an estimated value derived from a mathematical model, are used to make the network observable. Various techniques are used to forecast loads, such as support vector regression machines [19, 20], artificial neural networks [21, 22], hybridization of self-organized maps and support vector machines [23, 24], fuzzy-logic decision approach [25], linear regression [26],

and k-means [27]. These methods use historical load data and other related information, for example, weather conditions, to train the forecaster [19–23] or build a liner regression model [26]. In addition, the model-based method presented in [28], which constructs load models for each building, was used to estimate loads. This method might give a good estimation if all building types are thoroughly studied, but this is a really tough task for a meshed secondary network.

Smart meters can also be installed to help providing more information [29, 30], and their effectiveness was tested in small network, such as network with 8 loads [31], 110 houses [32], and 400 meters [33]. However, it is not (yet) possible to install smart meters at the connection points of every customer.

So far, the solutions mentioned above cannot be directly used to estimate loads in a heavily meshed secondary network (HMSN) due to the following points:

(1) An HMSN is a very typical complex power network and a low-voltage network where the loads are fed by network transformers connected at the secondaries. Only at the substation and the network transformers we can obtain the available real-time measurements, which are obtained from the SCADA at the substation and the remote monitoring system (RMS) at the secondary of the network transformers.

(2) The available measurements in a distribution system are not always enough to estimate the loads. This situation is the most adverse when trying to estimate the loads of an HMSN, in which load measurements are not normally available. This means that there are no historical load measurements as pseudomeasurements to start the state estimation process. Thus, load estimation of an HMSN is an extremely challenging task. This problem motivates this research.

(3) Device placement is widely used at the high and medium voltage levels [34–36]. The installation of meters at the low-voltage level is still very limited due to the high cost [31, 37]. In addition, the cost of smart meters also prevents their universalization in low-voltage distribution networks.

(4) Meter placement and load forecasting are helpful to estimate loads in a distribution system. But they mainly focused on radial or weakly meshed systems [2, 29, 30, 38–42] due to high cost or lack of historical data.

To estimate loads of an unobservable HMSN, this paper proposes a load estimation method based on available network transformer measurements. The main contributions are as follows:

(1) This is the first attempt to find a way to estimate loads of a typical complex power network (namely, an HMSN) based on a limited number of transformer measurements and forecasted loads, instead of historical load measurements. The proposed method, which consists of three steps: network reduction, load forecasting, and state estimation, is inspired by our observations and analysis of the strong relationship existing among temperature, load consumption, and transformer measurements in a long-term investigation. The advantage of this method is the avoidance of complex relationship analysis among power demands and influential factors, such as weather condition, building insulation, and cooling/heating systems.

(2) A power-temperature curve derived from standard load shapes is introduced to forecast loads. The forecasting accuracy is enhanced by introducing the concept of effective temperature reflecting varied weather conditions.

(3) A weighting factor for the least-squares state estimation method is presented to make sure that every building provides an equivalent contribution in relative and absolute terms. This prevents for the errors to concentrate on large or small loads.

A real heavily meshed secondary network in New York City with 1040 buses is used to conduct experiments to verify the effectiveness of the proposed method.

The remainder of this paper is organized as follows. Section 2 states the problem to be solved. The three main steps, network reduction, load forecasting, and state estimation, are detailed in Sections 3–5, respectively. In Section 6, experimental results and analysis are presented. Finally, conclusions are drawn in Section 7.

2. Problem Statement

Low-voltage highly meshed secondary networks (HMSNs) are frequently used in densely populated metropolitan areas in North America to improve reliability. The unique characteristic of these networks is that the transformer secondaries are all tied together by a heavily meshed low-voltage network from where the loads are connected. In HMSNs, there are numerous parallel paths from the substation to the loads offering the greatest reliability amongst the currently used distribution system configurations. For example, the topology of a typical network is shown in Figure 1, where the secondary network is highly meshed, and the medium voltage (MV) distribution feeders are radial and each one contains 20 to 50 network transformers. For more details, the reader is referred to [16].

To clearly show the structure of an HMSN, Figure 2 provides a zoomed in version of the secondary network in Figure 1. In this figure, all buses in the network can be classified into three types: transformer, load, and connection bus. Transformers have measurements on the secondary side (see Figure 2). Through the RMS, utilities know the power flow on the transformers at 15 min intervals. These measurement points can be considered as generators in this paper since reverse power cannot be allowed by the network protectors [16]. The presence of distributed generators (DGs) in the network does not affect this assumption since DGs are not allowed to push power back to the primary by the network protectors. DGs are modeled as negative loads.

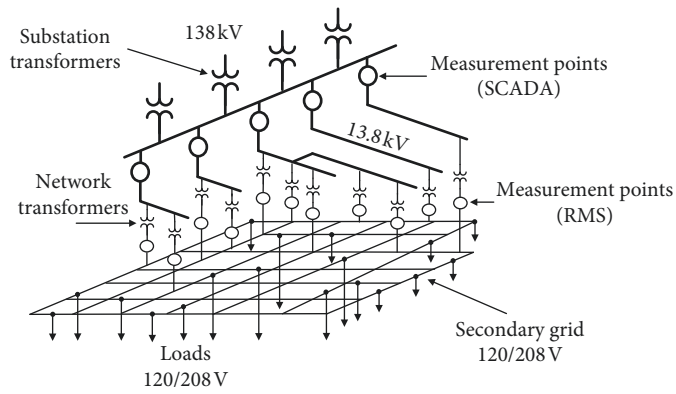

Figure 1: Topology of a typical secondary network. The secondary network is highly meshed. The only real-time measurements are the SCADA at the substation and the remote monitoring system (RMS) at the secondary of the network transformers.

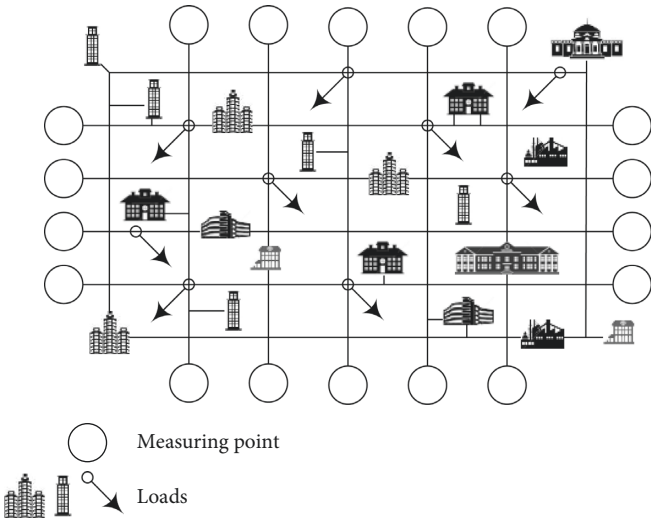

Figure 2: Schematic diagram of the secondary network in Figure 1.

The loads (buildings) only have measurement of energy averaged over 30 days. The problem consists in estimating the loads of this highly unobservable system for the 8760 hours of the year. Connection buses are those buses that only connect paths together, which have no loads or measurements. A typical network has hundreds of measuring points and thousands of unknown loads. It also has a substantial number of connection buses and multiple parallel connections between two buses.

There are almost no real-time or historical load measurements to ensure the observability of HMSNs. The observability of HMSN refers to the case when the number of measurements obtained is smaller than the number of measurements required by the state estimation. In this paper, as shown in Figure 2, only secondary transformers have real-time measurements. All the loads and connection buses have no real-time measurements. So, the HMSN is unobservable. A way to estimate unknown loads without the installation of additional meters is the use of available information at hand, which could be

(1) Real-time measurements of voltage, current, power, etc., from the remote monitoring system (RMS) at the secondary of the network transformers every 15 minutes

(2) Monthly consumer bills, measuring the energy averaged over a month

(3) Typical load shapes for each building type, which are obtained from measurements over several years of typical buildings

To estimate loads in such an unobservable secondary network, this paper proposes a load estimation method based on secondary transformer measurements without the installation of additional meters at loads. The method is composed of three main steps: network reduction, load forecasting, and state estimation. A schematic diagram of the proposed method is shown in Figure 3. First of all, the secondary network is mathematically reduced to load/measurement points terminals to make it suitable for state estimation. Subsequently, we introduce a method to forecast loads using available measurements, standard load shapes, and temperature. Finally, the forecasted loads regarded as pseudomeasurements and secondary transformer measurements are used to estimate the loads by using a state estimation algorithm.

3. Network Reduction

A real secondary network is far more complex than the one shown in Figure 2. As multiple parallel transmission lines between two buses are used to guarantee network reliability, many buses are used for connection. There are numerous connection buses without measurements in a real secondary network. For example, there are 505 connection buses in a 1040-bus network. Their existence greatly increases the computational burden of load estimation and may also cause estimation failure due to a large number of unknown buses. Furthermore, many spot networks in a secondary network can be considered as known loads since they are fed directly from 3 or 4 transformers. Therefore, it is necessary to reduce the network before load forecasting. The steps for network reduction are as follows:

(1) Merge parallel transmission lines between two buses

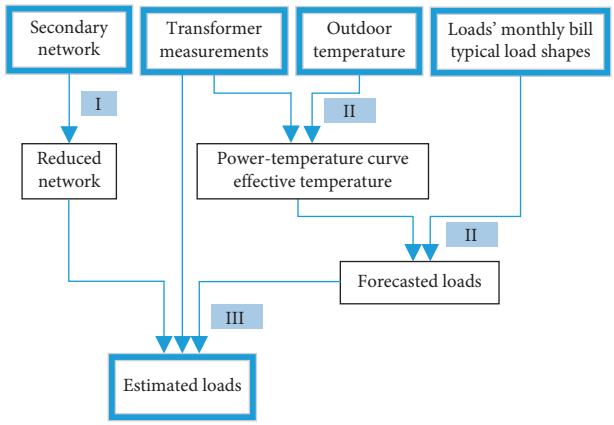

Figure 3: Schematic diagram of proposed load estimation method.

(2) Eliminate connection buses without measurement or load using Kron reduction [43]

(3) Remove spot networks from the network

The first and second steps are done mathematically accurately. Thus, the network reduction does not change the state (voltage magnitude and angle) of buses. The third step, spot networks removal, is done to eliminate the independent networks, which have no effect on the main grid. So, the network reduction does not change the accuracy of forecast.

4. Load Forecasting

This section discusses how to forecast loads in an HMSN as pseudomeasurements from available information at hand. In the considered HMSN, the available information consists of only transformer measurements, monthly customer bills, and typical load shapes at 15 min intervals and up to over one year. Therefore, the method is applicable for short-, mid-, and long-term load forecasting. Thus, to forecast loads from the very limited available information is a challenging problem [44–46].

To solve this problem, we look at the relationship between transformer measurements and weather conditions, from which a power-temperature curve could be obtained to forecast loads, together with loads' monthly bills and typical load shapes. As usual, the outdoor temperature is the main factor affecting power consumption; at the same time, building types and other weather conditions such as solar radiation also have an influence on the power consumption to a certain degree. To reflect the real case of power consumption, an improved outdoor temperature, called effective temperature, is introduced to forecast unknown loads.

In this section, we first introduce a forecasting method in Section 4.1 and then describe the load forecasting algorithm in Section 4.2.

4.1. Forecasting Method. To get the desired forecasting results, first the actual data of transformers and temperature are analyzed, and then a mathematical relationship between power and temperature called power-temperature curve (PTC) is derived. Using the derived PTC and outdoor temperature, the load shape of a transformer can be forecasted. Then, a weather influence factor called effective temperature is introduced to replace the outdoor temperature to obtain the load shape that matches well with real transformer measurements. This investigation indicates the feasibility and effectivity of the forecasting method. The method is used to forecast unknown loads in the next section.

The main idea of the proposed forecasting method can be described by using the following main steps:

(1) Collection and analysis of the actual data of transformers and outdoor temperature of the HMSN under research

(2) Correlation analysis between power and outdoor temperature

(3) Derivation of the power-temperature curve

(4) Verification and analysis of power-temperature curve

(5) Rectification for outdoor temperature

The steps are detailed one by one next.

4.1.1. Collection and Analysis of the Actual Data. Transformer load data are collected from a real secondary network [16]. The sampling time interval is one hour. Temperature data are obtained from a weather forecast website [47]. For example, we have collected and analyzed the data of a network transformer in an HMSN in 2010. Figure 4 shows the yearly load shape and the outdoor temperature.

4.1.2. Correlation Analysis between Power and Outdoor Temperature. To analyze the correlation between power and temperature, the load shape data are classified into 4 different day types: weekday, Saturday, Sunday, and National Public Holiday. The relationship among power consumption, temperature, and time of the day with respect to the weekday is illustrated in Figure 5, where a very clear correlation between temperature and power can be observed. There is a valley at around 50°F (10°C), from which the power changes as the temperature increases or decreases. This phenomenon can also be observed roughly in Figure 4. The peak of electrical power appears on the hottest day in July, when air conditioners are running at full capacity. The valley appears in the spring and fall, when cooling and heating systems are not used. One can observe from Figure 5 that the correlation between power and temperature changes with the time of the day. This results from several reasons: (1) in residential buildings, the temperature setting of cooling or heating systems varies during the day; (2) in some commercial buildings, the cooling and heating systems are turned on/off at given times, which causes a rapid power increase at the beginning of business hours; (3) the weather conditions such as strong solar irradiation or high humidity

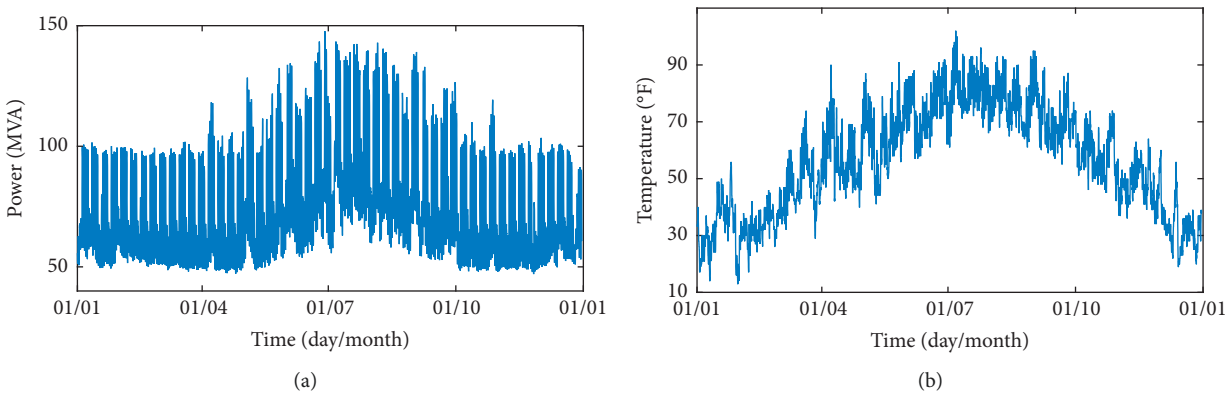

Figure 4: Actual load shape and outdoor temperature of one substation in NYC for 2010: (a) load shape; (b) outdoor temperature.

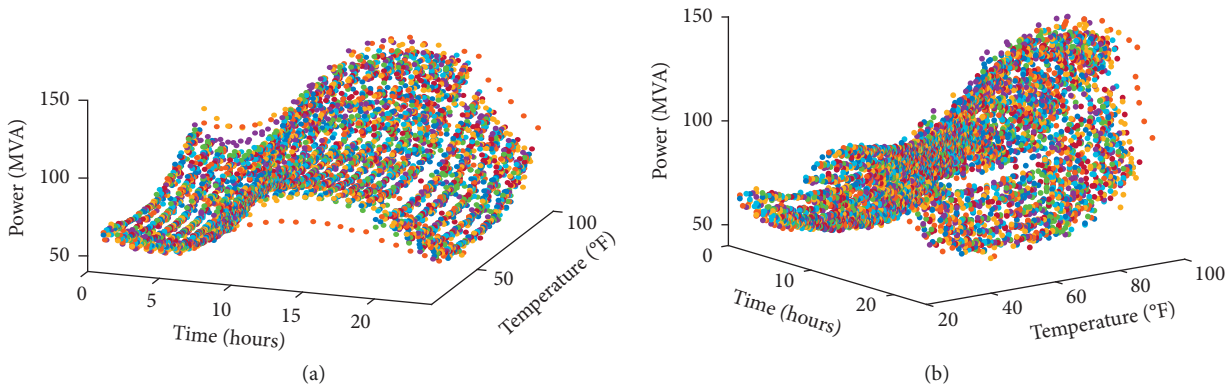

Figure 5: Relation between power consumption, temperature, and time of the day for all weekdays of 2010: (a) front view; (b) side view.

are also important factors, which cause the air conditioners to work harder early afternoon in the summer days.

According to the analysis of the relationship between power consumption, temperature, and time of the day, the behavior of power versus temperature at 2 AM and 11 AM is plotted in Figure 6, respectively.

4.1.3. Derivation of the Power-Temperature Curve. It is observed from Figure 6 that except for Holiday data, there is a parabolic curve-like distribution, which can be easily approximated by a third-order polynomial function. This is called the power-temperature curve (PTC) in this paper and is shown with solid lines in Figure 6. It is worth pointing out that the third-order polynomial function is a proper curve-fit technique here by trading off the performance and complexity of several popular methods like neural networks, support vector machines, and hybrid approaches.

To make the power-temperature curve easy to use, it needs to be normalized. According to our investigation, it is a good choice to consider the power at the almost lowest temperature 50°F (10°C) to perform the normalization because this point suffers less influence from cooling or heating systems. The normalization is formulated as

$$P_{\text{Nom}}(T,t) = \frac{P(T,t) - P(T_{\text{Base}},t)}{P(T_{\text{Base}},t)}, \quad (1)$$

where P_{Nom} is the normalized power, T is temperature, t is the time of a day, and T_{Base} is the base temperature, which is set to 50°F in this paper.

As usual, the normalized power-temperature curves slightly vary with networks (also buildings), the time of the day, and day types, but each of them can be well approximated by a third-order polynomial function. This can also be observed in Figure 7, where the normalized power-temperature curves of four networks are shown. Once the power-temperature curve is obtained, it can be used to forecast the load shape using standard day load shapes and outdoor temperatures.

4.1.4. Verification and Analysis of the Power-Temperature Curve. To test the effectiveness of the obtained power-temperature curve, a yearly load shape is forecasted based on the standard day load shape and temperature recordings in 2010. Here, we select three days, March 22, March 27, and March 28, when the temperature was around 50°F, as standard day load shapes for weekday, Saturday, and Sunday. Figure 8 shows the comparisons between the original and the forecasted load shapes. The forecasted load shape is very close to the original one at the valley, which verifies the effectiveness of the power-temperature curve. We also note, however, that the differences between the original and computed load shapes are slightly larger for the peak time,

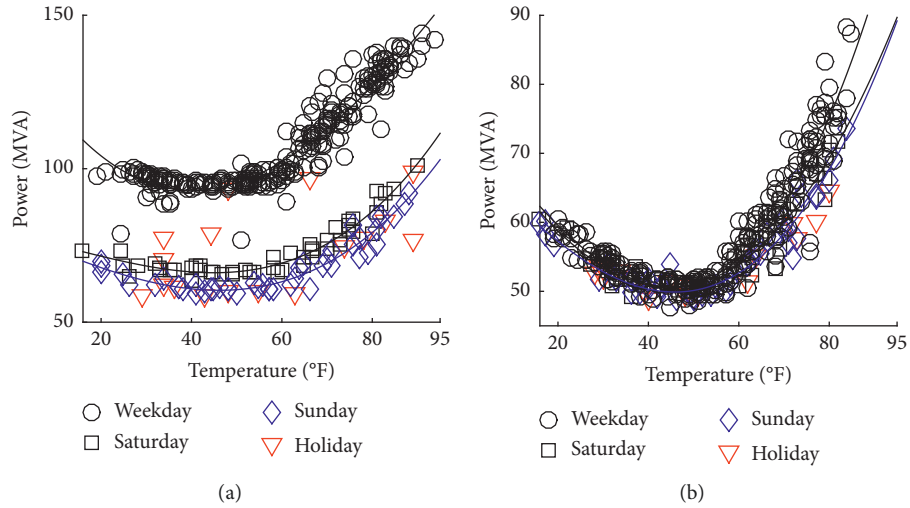

Figure 6: Power-temperature relation of one substation in 2010: (a) power-temperature relation at 11 AM; (b) power-temperature relation at 2 AM.

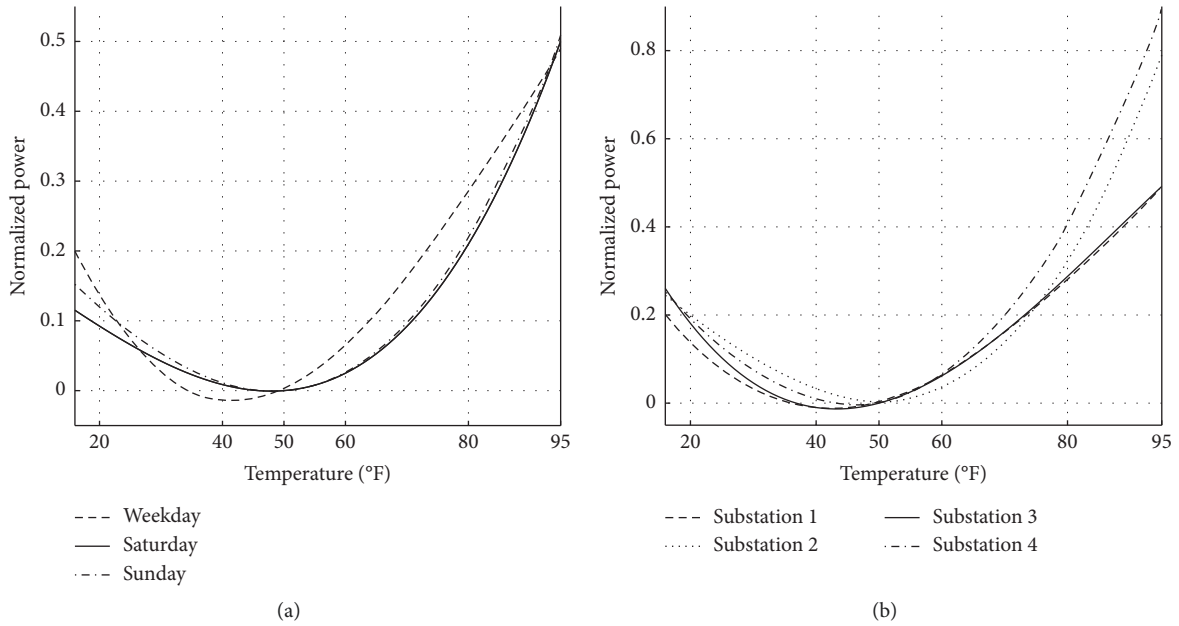

Figure 7: Normalized power-temperature curve of different network substations at 2 PM (power normalized based on 50°F): (a) curves for different day types of one substation; (b) curve for 4 substations of weekday.

when weather conditions are more complex. This deviation can be further rectified by introducing an effective temperature, which can reflect weather condition, not just outdoor temperature.

4.1.5. Rectification for Outdoor Temperature. According to the test and analysis of TPC, there is a little bias at the peak time, due to the complex weather conditions. In this research, the weather conditions are the concepts with a general meaning and represent the concentrated influence of many factors such as building type, building thermal insulation, temperature, solar radiation, rain, humidity, and wind speed. These factors are not decided by consumers themselves and mainly related to the weather conditions. We name them weather influence factors. The relations among weather influence factors are very complicated and therefore it is very difficult to derive a definitely mathematical formulation for load forecasting. Several investigations about the relation between weather conditions and loads were made in [26, 33] based on historical data of loads. It is worth noting that historical data of loads are not available in this research.

To reduce the bias, the concept called effective temperature reflecting various weather conditions is introduced to rectify the outdoor temperature. Effective temperature

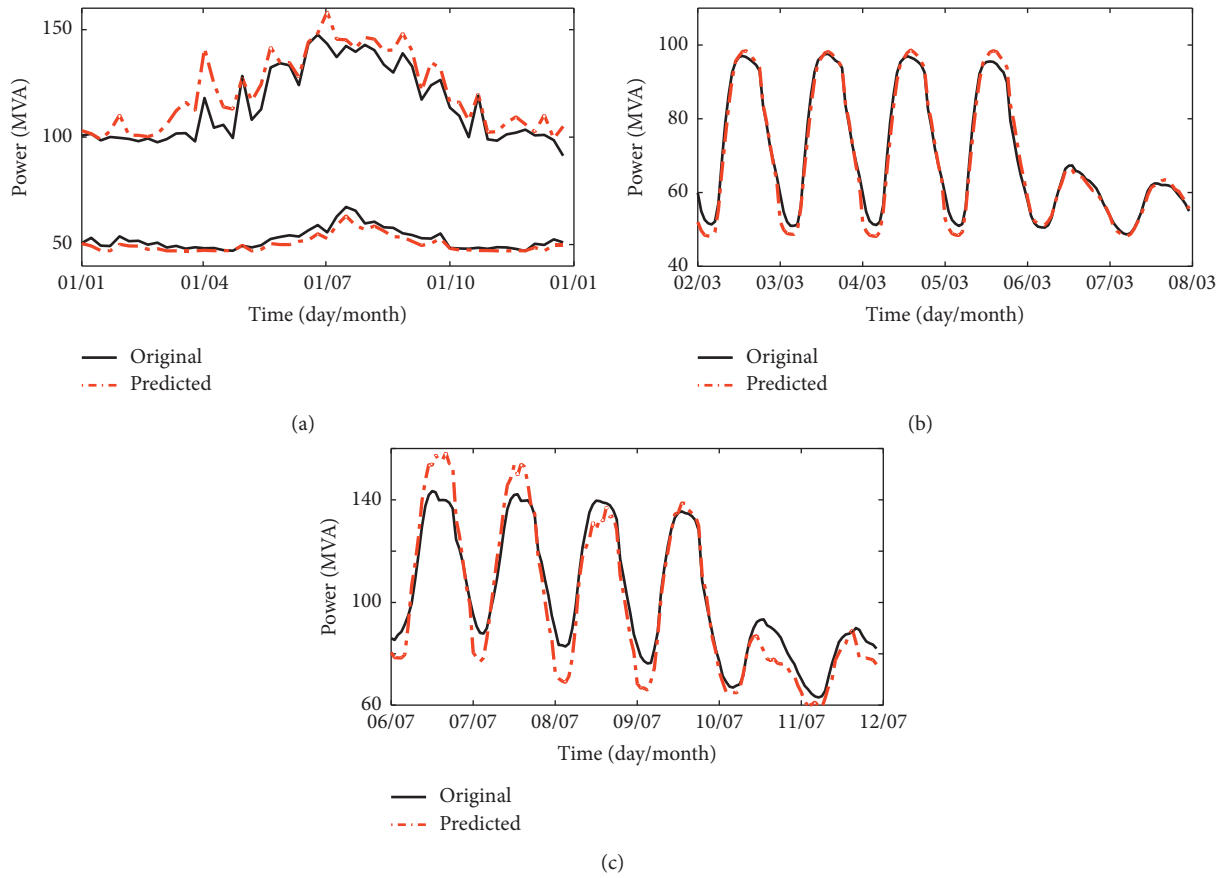

FIGURE 8: Comparison between the original load shapes and forecasted load shapes based on outdoor temperature: (a) envelope of the entire year; (b) valley; (c) peak.

can well represent the effect of outdoor weather conditions on the duty cycle of heating/cooling systems. It is known that the indoor comfort conditions depend on the outdoor temperature, humidity, pressure, wind speed, sunshine strength, building thermal insulation, and so on. An attempt about the use of the effective temperature is made to represent how much the power of heating/cooling systems would be affected by various weather conditions.

In what follows, real secondary transformer measurements are used to obtain effective temperature by rectifying the outdoor temperature. To obtain the effective temperature, the power-temperature curve is first obtained by a polynomial regression as shown in Figure 6, and then actual secondary transformer measurements are projected on the power-temperature curve. Thus, the corresponding effective temperature can be obtained. For example, suppose that the solid line in Figure 9 is a temperature-power curve obtained, where point A denotes a real measurement with power P_A and its corresponding outdoor temperature is T_A. The projected point of A is point B on the power-temperature curve. So, T_B is the effective temperature at point A.

To show the reasonableness of the effective temperature, Figure 10 compares the introduced effective temperature with outdoor temperature under different weather conditions. When it is clear, the effective temperature approximates the outdoor temperature. But when the weather

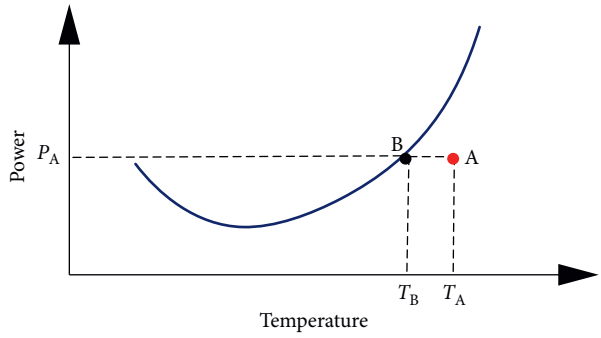

FIGURE 9: Effective temperature transition schematic graph.

conditions change drastically such as rain, the outdoor temperature will drop rapidly. In contrast to outdoor temperature, the effective temperature drops more smoothly and maintains at an average temperature, which is much closer to the actual situation. Figure 11 shows the forecasted load shape based on effective temperature. Comparing it with outdoor temperature in Figure 8, we can find that the effective temperature produces the load shapes more closely to the real load shape than outdoor temperature.

The effective temperature might be affected by random changes of loads or regression errors. Fortunately, there are many sources to get the effective temperature in one

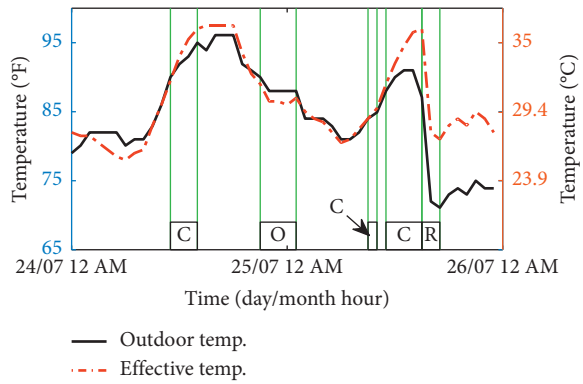

Figure 10: Relation between temperature and weather conditions: C, O, and R represent cloudy, overcast, and rain, respectively; the rest is clear.

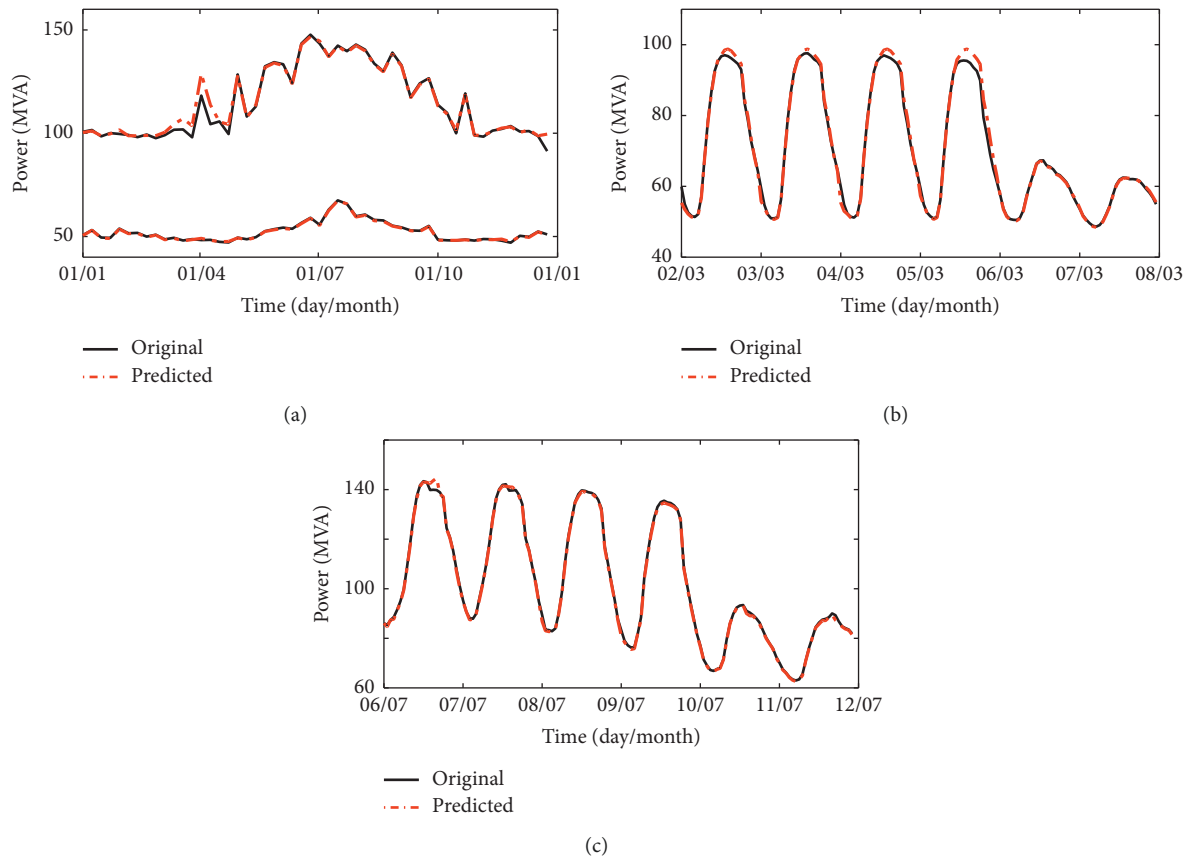

Figure 11: Comparison between the original load shapes and forecasted load shapes based on effective temperature: (a) entire year load shape envelope; (b) valley; (c) peak.

secondary network, e.g., there are 142 secondary transformers in the HMSN considered in this paper. The mean value of these effective temperatures can be used to largely decrease the uncertainty.

4.2. Load Forecasting Algorithm. In Section 4.1, the proposed forecasting method has been verified by the actual data of transformers. Different from transformers in an HMSN, load measurements are not available and what we can obtain are typical load shapes for various building types and monthly customer bills. Typical load shapes include several day load shapes, which correspond to different temperature intervals, respectively. These typical load shapes are too rough to be pseudomeasurements, but they can be used to derive PTC, which could be combined with effective temperature to forecast loads. On the other hand, local weather conditions have similar influence on the secondary transformer measurements and loads because both transformers and buildings in an HMSN are located within a relatively small geographical

area. Thus, the effective temperature derived from the TPC of transformers can also be used to construct load shapes of buildings. The steps for forecasting loads are as follows:

(1) Obtain typical load shapes with respect to building types and monthly bills

(2) Derive the power temperature curve by using the approach described in Section 4.1

(3) Combine the PTC with the effective temperature found from transformers in Section 4.1 to obtain normalized load shapes

(4) Scale the normalized load shapes using monthly bills

(5) Compute the loads from the scaled load shapes

It is worth pointing out that the spatial electric load forecasting by considering weather impacts was discussed for power delivery system planning in [46]. In this book, Chapter 5 analyzed the weather's impact on electric load for electricity demand and energy usage and developed equations to draw peak electricity demand for transmission and distribution planning based on statistical analysis. Chapter 6 further discussed the extreme weather that causes peak demand, while in this paper, there are two important points that are different from [46]: (1) the secondary distribution network is an unobservable network due to the lack of real-time load measurements; (2) although the historical weather data can be obtained from some public website, there are no historical load measurements except for monthly bills. The secondary network considered in this paper is always located in a "subarea" and is affected by "microclimates." The "effective temperature" is first derived from the secondary transformers and then is used to forecast loads. Following the load forecasting, the state estimation is used to obtain a more accurate estimation of all loads.

5. State Estimation

In Section 4, a forecasting method is introduced to forecast loads to be pseudomeasurements. Unlike transformer measurements, the pseudomeasurements are the approximation values of real measurements and can effectively solve the unobserved problem of HMSN as shown in Figure 2. If the voltage magnitudes and angles of points are carefully adjusted to satisfy power flow equations, the deviation between pseudomeasurements and real measurements could decrease step by step. Thus, in this section, a state estimation technique is used to compute loads by adjusting appropriate voltage magnitudes and angles of all points by iteration.

The basic idea of state estimation is to use meter measurements, which may not be accurate or have errors, to estimate the state vectors (voltage magnitude and angle) [48–51]. This can be formulated as the following minimization problem:

$$\min \sum_{i=1}^{M} \left[z_i - h_i(\mathbf{x})\right]^2, \tag{2}$$

where z_i is the i^{th} measurement, h_i is the corresponding estimated value, M is the total number of measurements, and $\mathbf{x}$ is the state vector, which consists of voltage magnitudes and angles. In a network with N buses, $\mathbf{x} = [|v_1|, |v_2|, \ldots, |v_N|, \theta_2, \ldots, \theta_N]^{\mathrm{T}}$. $\theta_1 = 0$ is chosen as the arbitrary reference angle.

Measurements have different accuracies, and each one is usually assigned a weight factor. The more accurate the measurement is, a larger weight is assigned. This is the so-called weighted least square (WLS) state estimation [52, 53], formulated as follows:

$$\min J(\mathbf{x}) = \left[z_i - h_i(\mathbf{x})\right]^{\mathrm{T}} \mathbf{W} \left[z_i - h_i(\mathbf{x})\right], \tag{3}$$

where $J(\mathbf{x})$ is the objective function and $\mathbf{W}$ is the weighting factor matrix. This equation is solved using the Gauss–Newton iterative method. State vector $\mathbf{x}$ is updated at each iteration using

$$\Delta\mathbf{x} = \left(\mathbf{H}^{\mathrm{T}}\mathbf{W}\mathbf{H}\right)^{-1} \mathbf{H}^{\mathrm{T}}\mathbf{W}\left[z - h(\mathbf{x})\right], \tag{4}$$

where $\mathbf{H}$ is the Jacobian matrix of $h(\mathbf{x})$. The iterations continue until $J(\mathbf{x})$ is smaller than a preset convergence criterion. The detailed procedure can be found in [19].

Once the state vector is obtained, the voltage magnitude and angle of each bus and the load can be calculated using the power flow equations. To start the state estimation process, the initial value of $\mathbf{x}$ is set as (flat start): $|v_i| = 1$, $\theta_i = 0$. The results of $\mathbf{x}$ obtained from the previous time are used as the initial values for the next time. This technique can greatly reduce the computation time.

The weighting matrix $\mathbf{W}$ in (4) is a diagonal matrix, defined as $\mathbf{W} = \mathrm{diag}\ [w_1, w_2, \ldots, w_N]$, where w_i is the weighting factor corresponding to the i^{th} measurement, and is set to $w_i = (\sigma_i^2)^{-1}$ in [19], where σ is the standard deviation of the i^{th} measurement.

Suppose that the measurements follow a Gaussian distribution. Therefore, three standard deviations ($\pm 3\sigma$) about the mean value account for over 99% of the area under the curve. Thus, the standard deviation for a given error is computed as [54, 55]:

$$\sigma_i = \frac{\mu_i \times \%\text{error}}{3 \times 100}, \tag{5}$$

where μ_i is the mean of the i^{th} measurement and %error is the corresponding maximum error.

As usual, the real-time measurements from secondary transformers are very accurate and should be assigned a large weighting factor, namely, a small standard deviation σ, while the pseudomeasurements from buildings measurements are forecasted values, which may not be accurate, and should be assigned a small weighting factor. Thus, the setting in (5) is not suitable for this kind of measurements. This is because the buildings in a secondary network always have different power demands, e.g., some demands are very large, hundred kW, while the others are very small, only a few kW. If we use (5), all buildings will get the same relative estimation error, but different absolute estimation errors. For example, if the relative estimation error is 10%, the absolute estimation errors will be 0.1 and 10 for buildings with powers 1 kW and 100 kW, respectively. To decrease the absolute estimation error for the buildings with large power demand,

we propose a modified weighting factor σ' to balance the absolute estimation and relative errors. σ' is defined as

$$\sigma_i' = \frac{\sqrt{\mu_i} \times \%\text{error}}{3 \times 100}. \quad (6)$$

The difference between σ' in (6) and σ in (5) can be observed in Figure 12. It is clear that σ' increases slower than σ as the mean value of measurements increases through adding a square root operation.

The pseudocode algorithm for the state estimation is illustrated in Figure 13, where z_i represents real-time measurements for secondary transformer buses (P, Q, V) and pseudomeasurements for load buses (P, Q); the weighting factor σ_i' corresponds to each measurement Z_i; the static vector $\mathbf{x}^k = [|v_1|, |v_2|, \ldots, |v_N|, \theta_2, \ldots, \theta_N]^{\mathrm{T}}$.

From Figure 13, the computational complexity of this algorithm can be analyzed. The steps before the WHILE loop have the time complexity O(N). Steps (vi) and (vii) have the time complexity O(N^2). Thus, the state estimation algorithm has the time complexity O(N^2).

It is worth pointing out that the topology of the model is considered to be accurate in this research. If there are missing or wrong data of buses, the estimation accuracy will decrease. In fact, the system is an unobservable network. If the disturbance comes from the real-time measurements of transformers, a relatively larger influence may occur, due to the larger weights. On the other hand, if the disturbance comes from the pseudomeasurements of loads, which are forecasted based on long observations, the model is not sensitive to the disturbance, due to the smaller weights.

6. Experiment

In this section, a real highly meshed secondary network in NYC is used to test the effectiveness of the proposed method. The results of network reduction are first provided to show its feasibility. Then, the comparisons of estimation errors are given to verify the effectiveness of the modified weighting matrix. Finally, estimation results are shown.

6.1. Results of Network Reduction. To illustrate the feasibility of network reduction, a relatively small network in New York City presented in [16] is used as example to conduct the experiment. The original network consists of 311 load buses, 244 transformers, 505 connection buses, and 3354 cable sections, which are listed in Table 1. The method described in Section 4 is used to reduce the network. The reduced numbers of load buses, transformers, connection buses, and cable sections are also listed in Table 1. The reduced network is much simpler than the original one.

6.2. Results of Modified Weighting Factor. In this section, the simulation data described in Section 6.3 are used to conduct the experiments to show the reasonableness of the modified weighting factor σ' in (6). The weighting factor σ in (5) and constant weighting factor σ'' (larger values for transformer measurements and smaller values for pseudomeasurements) are also considered to make a comparison.

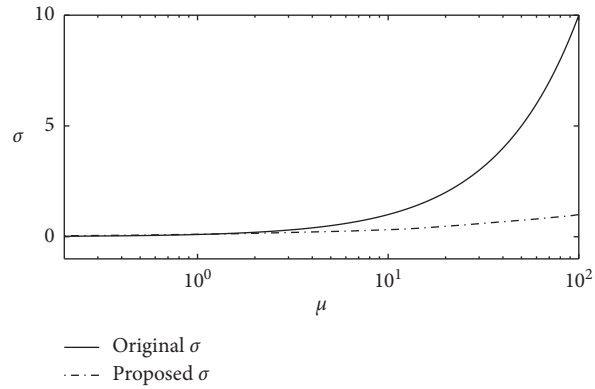

Figure 12: Difference between σ' in (6) and σ in (5) according to mean values of measurements.

Begin
(i) Set measurements z_i
(ii) Calculate weighting factor σ_i' using (6)
(iii) $k = 0$
(iv) Initialize the static vector $\boldsymbol{x}^k$
(v) **While** (max$\Delta\mathbf{x}$> a preset criterion ε) do
(vi) Calculate the estimated value $h(\boldsymbol{x}^k)$ and its Jacobian matrix $\boldsymbol{H}(\boldsymbol{x}^k)$
(vii) Calculate $\Delta\boldsymbol{x}$ using (4)
(viii) $\mathbf{x}^{k+1} = \mathbf{x}^k + \Delta\mathbf{x}^k$
$k = k + 1$
End
(ix) Calculate real and reactive power of loads using power flow based on $\boldsymbol{x}^{k+1}$
End

Figure 13: Pseudocode algorithm for the state estimation.

Table 1: Reduced results of a real small network in New York City.

Networks	Load buses	Transformers	Connection buses	Cable sections
Original	311	224	505	3354
Reduced	284	142	0	322

The results for the three weighting factors are shown in Figure 14.

It can be seen from Figure 14 that the modified weighting factor σ' in (6) has smaller absolute errors than the weighting factor σ in (5) as shown in Figure 14(a) and has smaller relative errors than the factor σ'' as shown in Figure 14(b). These results indicate that the modified weighting factor has a better tradeoff between relative and absolute errors than the other two weighting factors.

6.3. Estimating Results. To accomplish load estimation for a highly meshed secondary network in which only transformers' measurements, monthly bills, and typical load shapes are available, we follow the three steps illustrated in

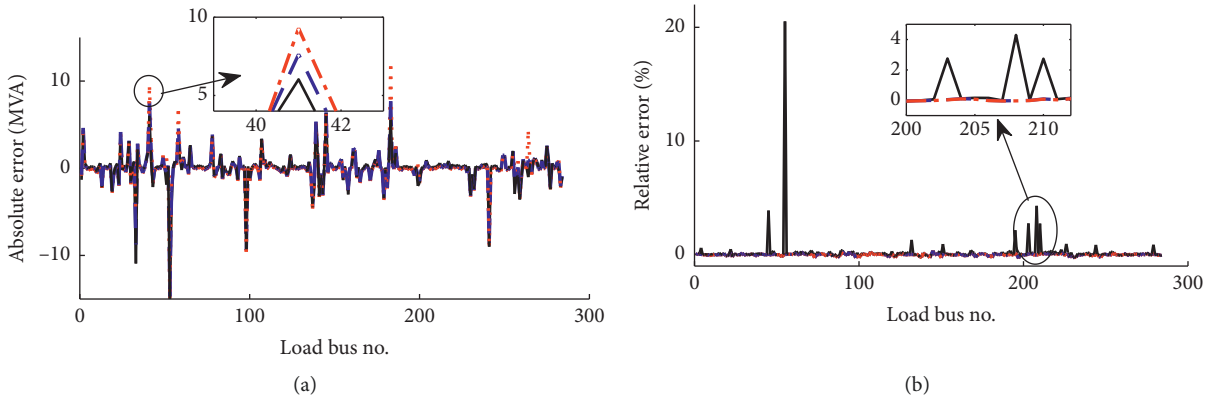

Figure 14: Estimation errors obtained by σ (dash-dot), σ'' (solid), and σ' (dash): (a) absolute estimation error; (b) relative estimation error.

Figure 3: network reduction, load forecasting, and state estimation, to obtain the experimental results.

We first obtain the reduced network by following the steps described in Section 3. Subsequently, we use the available standard load shape to obtain the testing data. The detailed procedures are described as follows.

All buildings are classified by customer class. There are seven typical building types: residential, religious, small general, large general, public buildings, public and private, and electrically heated schools. For each building type, we have a standard day load shape for each season. To create realistic conditions, each building should have its own load shape. There are three steps, scaling, shifting, and smoothing, to modify the standard load shape and make it distinct for each building. Scaling uses a random value from 80% to 120%. Shifting is to move the curve one hour before or after with a probability 20%. Smoothing is applied to prevent unreasonable changes with time. The new value should be around the original value and is not larger or smaller than 20%. The modification process is shown in Figure 15. It is worth pointing out that the second step is only applied to residential and small general service in our simulation since other buildings such as schools and public building always have fixed opening hours and do not shift their loads randomly.

The modified load shape is combined with the power-temperature curve, which is derived from standard load shape, to create the yearly load shape for each building. The power-temperature curve is also randomly modified to make the data more realistic, as shown in Figure 16. The maximal deviation in the modified curve is less than 5% of the original curve. The obtained building yearly load shape is taken as the real-time measurements of the building and sent to a power flow simulation tool, OpenDSS in this case. Through solving the power flow problem, the measurements of secondary transformers and monthly bills of each building can be computed. These measurements are what we can achieve from the network and are used for the state estimation.

The produced testing data consisting of standard load shapes, secondary transformer measurements, and monthly bills are used for state estimation. The absolute and relative estimation errors (absolute value) between the true load and

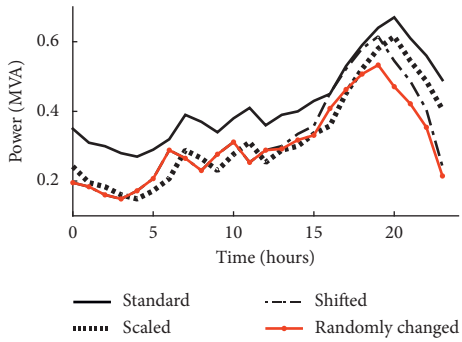

Figure 15: Modified load shapes (the standard load shape is residential weekday load shape).

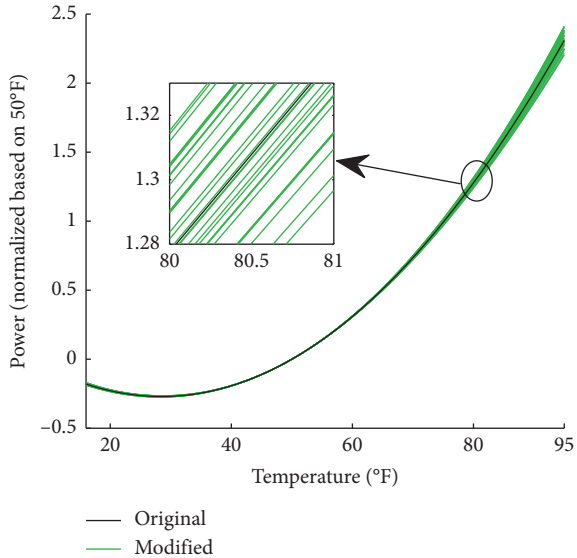

Figure 16: Modified power-temperature curve.

estimated load for all the buses at peak time (2:00 PM, July 6, 2010) are shown in Figure 17. The true values refer to the simulated power demands discussed above. These errors fall within an acceptable range and most loads have both small relative and absolute errors. The larger absolute estimation

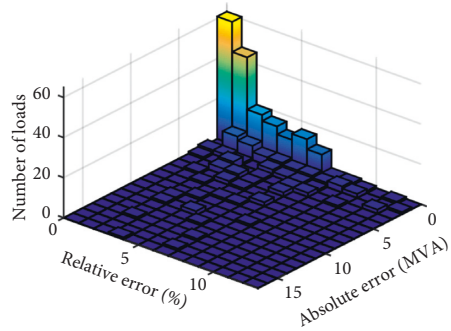

Figure 17: Comparisons of absolute and relative estimation errors (absolute value) between the true load and estimated load for all the buses at peak time (2:00 PM, July 6, 2010).

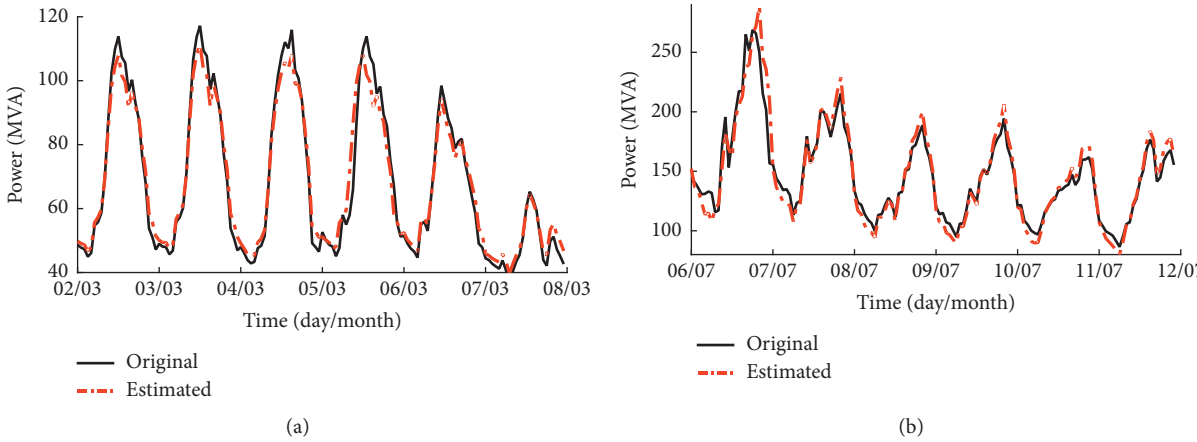

Figure 18: Comparison between original load shape and estimated load shape in one week for the load with the largest estimation error: (a) valley week; (b) peak week.

errors occur in the largest loads, but their relative estimation errors are small. Similarly, the smaller loads have small absolute estimation errors than others, even when their relative estimation error is a little larger. Figure 18 shows the comparison between the original loads shapes (namely true value) and the estimated load shapes for one week for the load with the largest estimation error. The absolute estimation errors of most buses are less than 5 MVA on the valley day and less than 10 MVA on the peak day when peak demand is nearly 300 MVA.

7. Conclusions

This paper has presented a method to estimate unobservable highly meshed secondary networks based on available transformer measurements, standard load shapes, and monthly bills. Experimental results of a real network in New York City show the feasibility and effectiveness of the proposed method in identifying hundreds of loads. This work indicates that the extremely challenging task, load estimation of highly meshed secondary networks, can be successfully solved by using the introduced method consisting of three steps: network reduction, load forecasting, and state estimation. We also introduced an effective temperature reflecting various weather conditions to rectify the outdoor temperature and a weighing factor to balance the absolute and relative errors of state estimation.

The proposed method is suitable for estimating loads of complex power loads in metropolitan areas, where the network topology is known and the secondary transformers are installed with measurements.

Future work will focus on the refinement of the state estimation methods used in the load estimation, such as computing complexity and the estimation robustness with respect to number of measurements, number of states, residuals in bad data detection, measurement error, parameter error, and topological error. Even the forecast approach or optimization techniques based on membrane computing could be considered [56–60].

Data Availability

The data used in this paper come from a specific complex power network. In response to the readers' requirements, the authors would consider sharing them.

Disclosure

Haina Rong was a visiting scholar in the Department of Electrical and Computer Engineering at New York

University, Brooklyn, NY, 11201, USA. (e-mail: ronghaina@126.com).

Conflicts of Interest

The authors declare that they have no conflicts of interest.

Acknowledgments

This work was supported in part by the National Natural Science Foundation of China (61702428, 61672437, and 61972324), Artificial Intelligence Key Laboratory of Sichuan Province (2019RYJ06), Sichuan Science and Technology Program (2018GZ0086 and 2018GZ0185), and New Generation Artificial Intelligence Science and Technology Major Project of Sichuan Province (2018GZDZX0043).

References

[1] U. Singh, V. Zamani, and M. Baran, "On-line load estimation for distribution automation using AMI data," in *Proceedings of the 2016 IEEE Power and Energy Society General Meeting (PESGM)*, pp. 1–5, Boston, MA, USA, July 2016.

[2] J. Wan and K. N. Miu, "Weighted least squares methods for load estimation in distribution networks," *IEEE Transactions on Power Systems*, vol. 18, no. 4, pp. 1338–1345, 2003.

[3] F. C. Schweppe, "Power system static state estimation," vol. 10, Report in the Power Systems Engineering Group, pp. 1–70, Massachusetts Institute of Technology, Cambridge, MA, USA, 1968.

[4] F. Schweppe and J. Wildes, "Power system static-state estimation, part I: exact model," *IEEE Transactions on Power Apparatus and Systems*, vol. PAS-89, no. 1, pp. 120–125, 1970.

[5] F. Schweppe and D. Rom, "Power system static-state estimation, part II: approximate model," *IEEE Transactions on Power Apparatus and Systems*, vol. PAS-89, no. 1, pp. 125–130, 1970.

[6] F. Schweppe, "Power system static-state estimation, part III: implementation," *IEEE Transactions on Power Apparatus and Systems*, vol. PAS-89, no. 1, pp. 130–135, 1970.

[7] D. Shirmohammadi, B. Wollenberg, A. Vojdani et al., "Transmission dispatch and congestion management in the emerging energy market structures," *IEEE Transactions on Power Systems*, vol. 13, no. 4, pp. 1466–1474, 1998.

[8] F. C. Schweppe and E. J. Handschin, "Static state estimation in electric power systems," *Proceedings of the IEEE*, vol. 62, no. 7, pp. 972–982, 1974.

[9] F. F. Wu, "Power system state estimation: a survey," *International Journal of Electrical Power & Energy Systems*, vol. 12, no. 2, pp. 80–87, 1990.

[10] J. Zhao, G. Zhang, and R. A. Jabr, "Robust detection of cyber attacks on state estimators using phasor measurements," *IEEE Transactions on Power Systems*, vol. 32, no. 3, pp. 2468–2470, 2017.

[11] J. Zhao, G. Zhang, K. Das et al., "Power system real-time monitoring by using PMU-based robust state estimation method," *IEEE Transactions on Smart Grid*, vol. 7, no. 1, pp. 300–309, 2016.

[12] J. Zhao and G. Zhang, "A robust prony method against synchrophasor measurement noise and outliers," *IEEE Transactions on Power Systems*, vol. 32, no. 3, pp. 2484–2486, 2017.

[13] M. E. Baran and A. W. Kelley, "State estimation for real-time monitoring of distribution systems," *IEEE Transactions on Power Systems*, vol. 9, no. 3, pp. 1601–1609, 1994.

[14] S. Meliopoulos, R. Huang, E. Polymeneas, and G. Cokkinides, "Distributed dynamic state estimation: fundamental building block for the smart grid," in *Proceedings of the 2015 IEEE Power & Energy Society General Meeting*, pp. 1–6, Denver, CO, USA, July 2015.

[15] A. Abur and A. Gómez Expósito, *Power System State Estimation: Theory and Implementation*, Marcel Dekker, New York, NY, USA, 2004.

[16] A. Bokhari, A. Raza, M. Diaz-Aguilo et al., "Combined effect of CVR and DG penetration in the voltage profile of low-voltage secondary distribution networks," *IEEE Transactions on Power Delivery*, vol. 31, no. 1, pp. 286–293, 2016.

[17] A. K. Singh and B. C. Pal, "Decentralized dynamic state estimation in power systems using unscented transformation," *IEEE Transactions on Power Systems*, vol. 29, no. 2, pp. 794–804, 2014.

[18] F. Aminifar, M. Shahidehpour, M. Fotuhi-Firuzabad, and S. Kamalinia, "Power system dynamic state estimation with synchronized phasor measurements," *IEEE Transactions on Instrumentation and Measurement*, vol. 63, no. 2, pp. 352–363, 2014.

[19] E. Ceperic, V. Ceperic, and A. Baric, "A strategy for short-term load forecasting by support vector regression machines," *IEEE Transactions on Power Systems*, vol. 28, no. 4, pp. 4356–4364, 2013.

[20] E. E. Elattar, J. Goulermas, and Q. H. Wu, "Electric load forecasting based on locally weighted support vector regression," *IEEE Transactions on Systems, Man, and Cybernetics, Part C (Applications and Reviews)*, vol. 40, no. 4, pp. 438–447, 2010.

[21] M. B. Tasre, V. N. Ghate, and P. P. Bedekar, "Hourly load forecasting using artificial neural network for a small area," in *Proceedings of the 2012 International Conference on Advances in Engineering, Science and Management*, pp. 379–385, Nagapattinam, India, March 2012.

[22] R. E. Abdel-Aal, "Short-term hourly load forecasting using abductive networks," *IEEE Transactions on Power Systems*, vol. 19, no. 1, pp. 164–173, 2004.

[23] S. Fan and L. Chen, "Short-term load forecasting based on an adaptive hybrid method," *IEEE Transactions on Power Systems*, vol. 21, no. 1, pp. 392–401, 2006.

[24] J. Llanos, R. Morales, A. Núñez et al., "Load estimation for microgrid planning based on a self-organizing map methodology," *Applied Soft Computing*, vol. 53, pp. 323–335, 2017.

[25] M. Rejc and M. Pantos, "Short-term transmission-loss forecast for the Slovenian transmission power system based on a fuzzy-logic decision approach," *IEEE Transactions on Power Systems*, vol. 26, no. 3, pp. 1511–1521, 2011.

[26] S. M. Moghaddas-Tafreshi and M. Farhadi, "A linear regression-based study for temperature sensitivity analysis of Iran electrical load," in *Proceedings of the 2008 IEEE International Conference on Industrial Technology*, pp. 1–7, Chengdu, China, April 2008.

[27] A. Al-Wakeel, J. Wu, and N. Jenkins, "*k*-means based load estimation of domestic smart meter measurements," *Applied Energy*, vol. 194, pp. 333–342, May 2017.

[28] Z. O'Neill, S. Narayanan, and R. Brahme, "Model-based thermal load estimation in buildings," in *Proceedings of the 2010 Fourth National Conf. of IBPSA-USA*, New York, NY, USA, August 2010.

[29] K. Vasudevan, C. S. R. Atla, and K. Balaraman, "Improved state estimation by optimal placement of measurement

devices in distribution system with DERs," in *Proceedings of the 2015 International Conference on Power and Advanced Control Engineering (ICPACE)*, pp. 253–257, Bangalore, India, August 2015.

[30] H. Wang and N. N. Schulz, "A revised branch current-based distribution system state estimation algorithm and meter placement impact," *IEEE Transactions on Power Systems*, vol. 19, no. 1, pp. 207–213, 2004.

[31] A. Abdel-Majeed and M. Braun, "Low voltage system state estimation using smart meters," in *Proceedings of the 2012 47th International Universities Power Engineering Conference (UPEC)*, pp. 1–6, London, UK, September 2012.

[32] D. Waeresch, R. Brandalik, J. Jordan, R. Bischler, W. H. Wellssow, and N. Schneider, "Linear state estimation in low voltage grids based on smart meter data," in *Proceedings of the 2015 IEEE Eindhoven PowerTech*, pp. 1–6, Eindhoven, Netherlands, June 2015.

[33] C. S. Chen, J. C. Hwang, Y. M. Tzeng, C. W. Huang, and M. Y. Cho, "Determination of customer load characteristics by load survey system at Taipower," *IEEE Transactions on Power Delivery*, vol. 11, no. 3, pp. 1430–1436, 1996.

[34] A. Ghassemian and B. Fardanesh, "Phasor assisted state estimation for NYS transmission system–implemention & testing," in *Proceedings of the 2009 IEEE/PES Power Systems Conference and Exposition*, pp. 1–8, Seattle, WA, USA, March 2009.

[35] A. T. Saric and R. M. Ciric, "Integrated fuzzy state estimation and load flow analysis in distribution networks," *IEEE Transactions on Power Delivery*, vol. 18, no. 2, pp. 571–578, 2003.

[36] J. Wu, Y. He, and N. Jenkins, "A robust state estimator for medium voltage distribution networks," *IEEE Transactions on Power Systems*, vol. 28, no. 2, pp. 1008–1016, 2013.

[37] W. H. Kersting, *Distribution System Modeling and Analysis*, CRC Press, Boca Raton, FL, USA, Electric Power Engineering Series, 2nd edition, 2006.

[38] V. Borozan and N. Rajakovic, "Minimum loss distribution network configuration: analyzes and management," in *Proceedings of the 14th International Conference and Exhibition on Electricity Distribution (CIRED 1997—Distributing Power for the Millennium)*, vol. 6, Birmingham, UK, June 1997.

[39] D. A. Haughton and G. T. Heydt, "A linear state estimation formulation for smart distribution systems," *IEEE Transactions on Power Systems*, vol. 28, no. 2, pp. 1187–1195, 2013.

[40] I. Dzafic, H. T. Neisius, and S. Henselmeyer, "Real time distribution system state estimation based on interior point method," in *Proceedings of the 17th Power Systems Computation Conference*, Stockholm, Sweden, August 2011.

[41] Y. Deng, Y. He, and B. Zhang, "A branch-estimation-based state estimation method for radial distribution systems," *IEEE Transactions on Power Delivery*, vol. 17, no. 4, pp. 1057–1062, 2002.

[42] H. Wang and N. N. Schulz, "A load modeling algorithm for distribution system state estimation," in *Proceedings of the 2001 IEEE/PES Transmission and Distribution Conference and Exposition*, vol. 1, pp. 102–105, Atlanta, GA, USA, November 2001.

[43] G. Kron, *Tensor Analysis of Networks*, Wiley, Hoboken, NJ, USA, 1939.

[44] B. Liu, J. Nowotarski, T. Hong, and R. Weron, "Probabilistic load forecasting via quantile regression averaging on sister forecasts," *IEEE Transactions on Smart Grid*, vol. 8, no. 2, pp. 730–737, 2017.

[45] W. Kong, Z. Y. Dong, D. J. Hill, F. Luo, and Y. Xu, "Short-term residential load forecasting based on resident behaviour learning," *IEEE Transactions on Power Systems*, vol. 33, no. 1, pp. 1087-1088, 2018.

[46] H. L. Willis, *Spatial Electric Load Forecasting*, Marcel Dekker, New York, NY, USA, 2002.

[47] http://www.wunderground.com/.

[48] J. Zhao, G. Zhang, M. L. Scala, and Z. Wang, "Enhanced robustness of state estimator to bad data processing through multi-innovation analysis," *IEEE Transactions on Industrial Informatics*, vol. 13, no. 4, pp. 1610–1619, 2017.

[49] J. Zhao, G. Zhang, Z. Y. Dong, and K. P. Wong, "Forecasting-aided imperfect false data injection attacks against power system nonlinear state estimation," *IEEE Transactions on Smart Grid*, vol. 7, no. 1, pp. 6–8, 2016.

[50] J. Zhao, G. Zhang, M. La Scala, Z. Y. Dong, C. Chen, and J. Wang, "Short-term state forecasting-aided method for detection of smart grid general false data injection attacks," *IEEE Transactions on Smart Grid*, vol. 8, no. 4, pp. 1580–1590, 2017.

[51] J. Zhao, Z. Wang, C. Chen, and G. Zhang, "Robust voltage instability predictor," *IEEE Transactions on Power Systems*, vol. 32, no. 2, pp. 1578-1579, 2017.

[52] H. Merrill and F. Schweppe, "Bad data suppression in power system static state estimation," *IEEE Transactions on Power Apparatus and Systems*, vol. PAS-90, no. 6, pp. 2718–2725, November 1971.

[53] A. Monticelli, "Modeling circuit breakers in weighted least squares state estimation," *IEEE Transactions on Power Systems*, vol. 8, no. 3, pp. 1143–1149, 1993.

[54] P. A. Pegoraro and S. Sulis, "On the uncertainty evaluation in distribution system state estimation," in *Proceedings of the 2011 IEEE International Conference on Smart Measurements of Future Grids (SMFG)*, pp. 59–63, Bologna, Italy, November 2011.

[55] R. Singh, B. C. Pal, and R. B. Vinter, "Measurement placement in distribution system state estimation," *IEEE Transactions on Power Systems*, vol. 24, no. 2, pp. 668–675, May 2009.

[56] T. Wang, G. Zhang, and M. J. Pérez-Jiménez, "Fuzzy membrane computing: theory and applications," *International Journal of Computers, Communications & Control*, vol. 10, no. 6, pp. 904–935, 2015.

[57] T. Wang, G. Zhang, J. Zhao, Z. He, J. Wang, and M. J. Perez-Jimenez, "Fault diagnosis of electric power systems based on fuzzy reasoning spiking neural P systems," *IEEE Transactions on Power Systems*, vol. 30, no. 3, pp. 1182–1194, 2015.

[58] G. Zhang, H. Rong, F. Neri, and M. J. Pérez-Jiménez, "An optimization spiking neural P system for approximately solving combinatorial optimization problems," *International Journal of Neural Systems*, vol. 24, no. 5, Article ID 1440006, 2014.

[59] G. Zhang, M. Gheorghe, L. Pan, and M. J. Pérez-Jiménez, "Evolutionary membrane computing: a comprehensive survey and new results," *Information Sciences*, vol. 279, pp. 528–551, 2014.

[60] G. Zhang, M. J. Pérez-Jiménez, and M. Gheorghe, *Real-life Applications with Membrane Computing*, Springer, Berlin, Germany, 2017.